Title: The influences of cultivation setting on inflorescence lipid distributions, concentrations, and carbon isotope ratios of *Cannabis sp*

Author: Brett J. Tipple Bastian Hambach Janet E. Barnette Lesley A. Chesson James R. Ehleringer

PII: S0379-0738(16)30115-3
DOI: http://dx.doi.org/doi:10.1016/j.forsciint.2016.03.029
Reference: FSI 8389

To appear in: *FSI*

Received date: 21-11-2015
Revised date: 3-3-2016
Accepted date: 8-3-2016

Please cite this article as: B.J. Tipple, B. Hambach, J.E. Barnette, L.A. Chesson, J.R. Ehleringer, The influences of cultivation setting on inflorescence lipid distributions, concentrations, and carbon isotope ratios of *Cannabis sp.*, *Forensic Science International* (2016), http://dx.doi.org/10.1016/j.forsciint.2016.03.029

Title Page:

The influences of cultivation setting on inflorescence lipid distributions, concentrations, and carbon isotope ratios of *Cannabis sp.*

Brett J. Tipple[1, 2*] [brett.tipple@utah.edu]
Bastian Hambach[1#] [b.hambach@noc.soton.ac.uk]
Janet E. Barnette[1] [janet.barnette@utah.edu]
Lesley A. Chesson[3] [lesley@isoforensics.com]
James R. Ehleringer[1, 2] [jim.ehleringer@utah.edu]

[1]Department of Biology, University of Utah, Salt Lake City, UT 84112
[2]Global Change and Sustainability Center, University of Utah, Salt Lake City, UT 84112
[3]IsoForensics Inc., Salt Lake City, UT, 84108

[*]Corresponding Author
[#]Current Institution: National Oceanography Centre, University of Southampton, Southampton, United Kingdom

Title: The influences of cultivation setting on inflorescence lipid distributions, concentrations, and carbon isotope ratios of *Cannabis sp.*

Abstract

While much is known about how the growth environment influences many aspects of floral morphology and physiology, little is known about how the growth settings influences floral lipid composition. We explored variations in paraffin wax composition in *Cannabis sp.*, a cash crop grown both indoors and outdoors across the United States today. Given an increased focus on regulation of this crop, there are additional incentives to certify the setting of *Cannabis* cultivation. To understand the impacts of the growth environment, we studied distributions, concentrations, and carbon isotope ratios of *n*-alkanes isolated from *Cannabis sp.* inflorescences to assess if variations within these lipid parameters were related to known growth settings of specimens seized by federal agents. We found that *Cannabis* plants cultivated under open field settings had increased

inflorescence paraffin wax abundances and greater production of lower molecular weight *n*-alkane relative to plants grown in enclosed environments. Further, the carbon isotope ratios of *n*-C_{29} from *Cannabis* plants grown in enclosed environments had relatively lower carbon isotope ($\delta^{13}C$) values compared to plants from open-field environments. While this set of observations on seized plant specimens cannot address the particular driver behind these observations, we posit that (a) variations in irradiance and/or photoperiod may influence the distribution and concentration of inflorescence lipids, and (b) the $\delta^{13}C$ value of source CO_2 and lipid concentration regulates the $\delta^{13}C$ values of inflorescence *n*-C_{29} and bulk *Cannabis* plant materials. Nonetheless, by using a cultivation model based on $\delta^{13}C$ values of *n*-C_{29}, the model correctly identified the growth environment 90 % of time. We suggest that these lipid markers may be used to trace cultivation methods of *Cannabis sp*. now and become a more powerful marker in the future, once the mechanism(s) behind these patterns is uncovered.

Key Words:
marijuana, eradicated specimens, stable isotopes, compound-specific isotope analysis, plant organs, *n*-alkanes, growth setting

1.0. Introduction

The policies surrounding the use and distribution of marijuana (*Cannabis sp.*) are controversial within the United States. While possession, cultivation, and sales of marijuana remains illegal under the Federal Controlled Substance Act, the District of Columbia and the States of Washington, Colorado, Oregon, and Alaska have recently legalized marijuana for personal use and additional States have current ballot measures. In response, the Department of Justice released a series of enforcement priorities seeking to avert the public health consequences of marijuana usage; curb trafficking and violence associated with illegal marijuana distribution and sales by criminal enterprises; and limit transport of marijuana between jurisdictions with differing marijuana laws. These District and State jurisdictions are now working to develop regulatory mechanisms for the production and sales of marijuana and other marijuana-derived products; however, given the nascent state of the legislation, there remain numerous ambiguities within these regulations. In particular, within jurisdictions where *Cannabis* production and sale is legal, the growth environments of *Cannabis* cultivation are highly regulated by the local government. As an example, the State of Colorado requires the physical locations of *Cannabis* cultivation—such as individual fields or specific glass/hothouses—as well as the site of production facilities to be certified and all crops and products must be inventoried. Thus, there is a need for product traceability during plant cultivation, harvest, shipment, and following the manufacture of *Cannabis* products.

Stable isotope analysis of marijuana has demonstrated its potential to improve the forensic and law enforcement communities' understanding of marijuana production methods, growth environments, and trafficking networks [1-3]. In this respect, carbon ($\delta^{13}C$) and nitrogen ($\delta^{15}N$) isotope values have proven moderately useful. In a series of papers, Shibuya and colleagues demonstrated the potential to differentiate three of the five major production regions of marijuana cultivation in Brazil based on observed differences in the bulk $\delta^{13}C$ and $\delta^{15}N$ isotope values of seized marijuana samples [4, 5]. West and others followed with a study of eradicated and seized material from the U.S., but could not to distinguish region-of-origin based on bulk $\delta^{13}C$ and $\delta^{15}N$ values alone [6]. While cultivation location could not be assigned in this dataset, the growth environment could be identified using $\delta^{13}C$ values as plants grown outdoors had unique values compared to plants grown in a greenhouse system [6].

In plants, stable carbon isotope ($\delta^{13}C$) values reflect the additive influences of the $\delta^{13}C$ value of atmospheric CO_2 and isotopic fractionations associated with diffusion and carbon fixation [7, 8]. These fractionation events depend on the ratio of the concentrations of atmospheric CO_2 inside (c_i) and outside (c_a) of the leaf. Given that the $\delta^{13}C$ value of atmospheric CO_2 and plant fractionation factors are relatively fixed, c_i/c_a is responsible for the majority of isotopic variability for a given species living in natural and managed environments [7, 8]. Factors influencing a plant's $\delta^{13}C$ value through variation in c_i/c_a are broadly related to plant-water relations and irradiance [7]. The c_i/c_a is responsive to changes in the stomatal conductance, with important influences on conductance being ambient water vapor deficit, soil moisture, and leaf temperature [9-

17]. Both field and laboratory studies have provided extensive evidence for the impact of plant-water relations and irradiance on $\delta^{13}C$ values in a variety of plant tissues [18-22]. However, there may be cases where bulk plant tissues are not available, particularly with drug compounds derived from plants, and there have been very few experiments carried out under semi-controlled conditions to understand how these processes effect the distributions of and $\delta^{13}C$ values of specific plant molecules [23-25].

Analysis of non-refractory *Cannabis sp.* compounds, particularly the cannabinoids and other terpenoids, has been an area of significant scientific research [26-28]. The distribution of cannabinoids have been used to discriminate between *Cannabis* strains and geographic origin of marijuana strains [29, 30]. Recently, compound-specific isotope analysis (CSIA) of the carbon isotope values of cannabinol (CBN), cannabidiol (CBD) and THC has been demonstrated as feasible [31]. However, it has been well documented that the distribution of cannabinoids can vary markedly within a single plant, through a plant's life cycle, as plant material ages, and within a single seizure collection [32-35]. These variations complicate the standardized usage of cannabinoid distributions and isotope ratios of these compounds as regulatory tools and illustrate the need for the development of a method using refractory, unchanging compounds to monitor and source *Cannabis* compounds.

High molecular weight straight chain alkanes (*n*-alkanes) are ubiquitous in higher plants including *Cannabis sp.* [36]. Furthermore, *n*-alkanes are highly refractory and are not altered by isotopic exchange at normal surface temperatures and pressures [37]. These

118 characteristics make *n*-alkanes a possible tool for the regulation and certification of
119 *Cannabis*-derived products.
120
121 Here, we present chain-length distributions, concentrations, and stable carbon isotope
122 compositions of *n*-alkanes extracted from *Cannabis* inflorescences seized by the U.S.
123 Drug Enforcement Agency (DEA) from clandestine growing operations employing either
124 enclosed, greenhouse systems or open field farming methods. This experimental design
125 allows us to investigate the impacts of cultivation method on plant waxes and we
126 hypothesized that cultivation method is recorded in *Cannabis* *n*-C_{29} carbon isotope ratios,
127 similar to the information recorded by bulk *Cannabis* materials [6, 38]. To test this
128 hypothesis, we analyzed 84 *Cannabis* inflorescences of U.S. origin from known
129 cultivation settings (i.e., enclosed system vs. open field environments) and explored the
130 association between growth settings and the distributions, concentrations, and $\delta^{13}C$ values
131 of *n*-C_{29}.
132

133 ## 2. Methods

134 ### *2.1. Sample localities and materials collected*

135 We analyzed inflorescences from 84 fully mature domestic marijuana samples of known
136 origin from 53 counties within 18 states (**Table 1**). Samples analyzed here are a subset of
137 materials used in studies by West et al. [6, 39] and Hurley et al. [38, 40]. In this study on
138 compound specific isotope analyses, samples were selected from 9 states where
139 possession and usage of marijuana is illegal (AR, FL, IN, KY, MO, TN, TX, WI, and
140 WV) and from 9 additional states with various state-level statutes ranging from legal

141 medical usage (HI, IL, and MT), medical and possession decriminalization (CA, NY, and
142 VT), and legalization (AK, OR, WA). *Cannabis* inflorescence, leaf material, stems, and
143 in some cases roots and seeds were collected between 2003 and 2006 through the U.S.
144 Drug Enforcement Administration's (DEA) eradication efforts. Notes were provided
145 reporting the growth setting (i.e., enclosed, open field) employed at the clandestine
146 growing operation for all specimens. In addition, information regarding number of plants
147 seized, approximate canopy-cover, and plant height was reported for some, but not all
148 samples. No information regarding the species or specific cultivar of *Cannabis* was
149 provided. Materials used in this study were collected from archived material that was
150 desiccated and stored in 4-ml glass vials at the University of Utah since initial sample
151 intake. Of the 84 samples, 62 of them were noted by the DEA as having been grown in
152 open field environments and 22 as having been cultivated within enclosed environments.
153

154 *2.2 Lipid extraction, identification, and quantification*

155 Samples (50-400 mg) of inflorescences were isolated and pulverized with a mortar and
156 pestle, filtering and regrinding residual large particles by passing ground material through
157 a 250-μm stainless steel sieve until all material was ground and homogenized. Lipids
158 were extracted from 100-300 mg of powdered inflorescences with 2:1 dichloromethane
159 (DCM)/methanol by ultra-sonication (30 min × 2). The resulting total lipid extracts were
160 concentrated under a stream of purified nitrogen using a FlexiVap Work Station (Glas-
161 Col, Terre Haute, IN, USA), transferred to 4-ml glass vials, and further evaporated under
162 a gentle stream of N_2 gas. Extracts were then separated into compound classes by column
163 chromatography using 1 g deactivated silica gel (70-230 mesh) in an ashed Pasteur

pipette, and eluted with 2 ml hexane to obtain the saturated hydrocarbons following Tipple and Pagani [41].

Compounds were identified and their abundances were quantified using a Thermo Ultra gas chromatograph (GC) fitted with a programmable-temperature vaporization (PTV) injector and flame ionization detector. Hydrocarbons were introduced to the PTV injector at 40°C, followed by a 50°C/sec ramp to 320°C. The GC oven temperature program utilized was 60-320°C at 15°C/min with a final isothermal stage lasting 30 min. Compounds were identified through comparison of elution times with *n*-alkane standards (*n*-C_{18}, *n*-C_{20}, *n*-C_{22}, *n*-C_{24}, *n*-C_{28}, and *n*-C_{32}). Compound concentrations were quantified using a 5-point calibration curve generated from reference materials (*n*-C_{24} and *n*-C_{28} analyzed together at 25 ng, 50 ng, 100 ng, 500 ng, 1000 ng).

2.3. Chain-length Distributions and Concentrations of n-alkanes

Peak areas of high molecular weight *n*-alkanes were measured in order to quantify distributions of *n*-alkanes. Carbon preference indices (CPI) were calculated following Marzi *et al.* [42]:

$$CPI = \frac{(A_{23} + A_{25} + A_{27} + A_{29} + A_{31} + A_{33}) + (A_{25} + A_{27} + A_{29} + A_{31} + A_{33} + A_{35})}{2(A_{24} + A_{26} + A_{28} + A_{30} + A_{32} + A_{34})} \quad \textbf{Equation 1},$$

where "A" represents the area of the individual *n*-alkane peak from the chromatograph trace.

To calculate the average chain length of *n*-alkanes from inflorescences, the following was used:

$$ACL = \frac{(A_{23}(23)) + (A_{25}(25)) + (A_{31}(27)) + (A_{29}(29)) + (A_{31}(31)) + (A_{33}(33)) + (A_{35}(35))}{(A_{23} + A_{25} + A_{27} + A_{29} + A_{31} + A_{33} + A_{35})} \quad \textbf{Equation 2}.$$

2.4 Compound-specific isotope analysis

Compounds were separated using a Hewlett Packard 6890A GC employing a split-splitless injector held at a constant 310°C with an GC oven temperature at 80°C, followed by a 6°C/min ramp to 320°C with an isothermal for 12 min. A fused silica, DB-1, phase column (30 m × 0.25 mm I.D., 0.25 μm film thickness; J&W Scientific, Agilent Technologies, Santa Clara, CA, USA) was used with helium as the carrier at a flow of 1.2 ml/min. Compounds were subsequently combusted over nickel oxide, copper oxide, and platinum at 1000°C and analyzed for carbon isotope ratios using a Thermo Finnigan Delta^{plus}XL isotope ratio mass spectrometer. Individual *n*-C_{29} isotope ratios were normalized to the VPDB scale using a two-point linear calibration of *n*-alkane standard reference materials, which had previously been standardized to the VPDB scale [*n*-C_{18} (–33.3 ‰) and *n*-C_{28} (–29.0 ‰)] and analyzed after every fifth unknown in an analytical sequence. Arndt Schimmelmann's "*Mix A4*" [*n*-C_{16} (–30.7 ‰), *n*-C_{17} (–31.2 ‰), *n*-C_{18} (–31.1 ‰), *n*-C_{19} (–33.2 ‰), *n*-C_{20} (–32.4 ‰), *n*-C_{21} (–29.1 ‰), *n*-C_{22} (–32.9 ‰), *n*-C_{23} (–31.8 ‰), *n*-C_{24} (–33.3 ‰), *n*-C_{25} (–28.5 ‰), *n*-C_{26} (–33.0 ‰), *n*-C_{27} (–29.6 ‰), *n*-C_{28} (–32.2 ‰), *n*-C_{29} (–30.1 ‰), and *n*-C_{30} (–29.9 ‰)] was analyzed twice in each analytical sequence (n = 32) and had an measured accuracy of 0.1 ‰. Precision for *n*-alkanes

208 carbon isotope determinations was ± 0.3 ‰ (1σ, n = 157), as determined from a co-
209 injected QC reference material [5α-androstane (–30.1 ‰)].
210
211 All isotopic compositions are calculated following:
212 $\delta = (R_{samp}/R_{std})$-1 **Equation 3**,
213 where R represents the $^{13}C/^{12}C$ abundance ratio, and R_{samp} and R_{std} represent the sample
214 and standard, respectively. Delta values are reported in per mil (‰) notation and are
215 expressed relative to Vienna Pee Dee Belemnite (VPDB).
216
217 The apparent carbon isotope fractionation between n-C_{29} and bulk inflorescence (ε_{app}) is
218 defined as:
219 $\varepsilon_{app} = (\delta^{13}C_{n\text{-}C29} + 1)/(\delta^{13}C_{Bulk} + 1)$-1, **Equation 4**.
220
221 The carbon isotope value of bulk inflorescence ($\delta^{13}C_{Bulk}$) used to determine ε_{app} were
222 previously analyzed and reported in West et al. [6]. Briefly, West and colleague analyzed
223 $\delta^{13}C_{Bulk}$ using an elemental analyzer coupled to a Thermo Scientific Delta^{plus} isotope ratio
224 mass spectrometer and used an offset correction from an known reference material to
225 calibrate the unknown to the VPDB scale. They reported an overall precision of ± 0.09 ‰
226 for $\delta^{13}C_{Bulk}$.
227
228 *2.5. Statistical analysis*
229

Statistical analysis was completed using JMP® 11 Pro (SAS; Cary, NC) and PRISM® 5.0c (Graphpad Software, Inc; La Jolla, CA) for Mac OS X. Normality of distributions was tested with the Shapiro-Wilkes test. If the distributions were normal, then the Welch *t*-test was used to compare means at $\alpha = 0.05$. If the distributions were not normally distributed, then the Wilcoxon/Kruskal-Wallis (Rank Sums) test was used to assess differences between growth settings at $\alpha = 0.05$.

The measured $\delta^{13}C$ values of paired *n*-alkane and bulk inflorescences were compared using total least squares regressions. Regression lines were fitted to data only when the slope of the line was significantly different from 0 at the $\alpha = 0.01$ level.

3. Results and Discussion

3.1 Compound distributions of n-alkanes on Cannabis inflorescence

Cannabis sp. produced *n*-C_{17} to *n*-C_{33} with *n*-C_{29} (929 ± 680 μg g^{-1}) being the most abundant homologue, approximately four-times more abundant than the next most abundant homologue, *n*-C_{27} (254 ± 242 μg g^{-1}) and five-times more abundant than *n*-C_{31} (178 ± 134 μg g^{-1}) (**Table 1**). We noted large variation in concentrations of *n*-alkanes between individual specimens (**Table 1**). These variations are most likely due to differences in *Cannabis* species or cultivars. Nonetheless, significant differences between the concentrations of *n*-C_{29} for the two growth settings—enclosed versus field environments—were detected [Wilcoxon/Kruskal-Wallis, $W(91.2) = 3.781$, $z = -2.925$, $p = 0.0034$], where the plants grown in field environments had a significantly greater

253 concentration of *n*-C_{29} (1041 ± 743 μg g^{-1}) compared to the plants grown in enclosed
254 environments (614 ± 290 μg g^{-1}). Significant differences between the concentrations of
255 total *n*-alkanes for the two growth settings were also detected [Wilcoxon/Kruskal-Wallis,
256 $W(82.0) = 3.997$, $z = -3.098$, $p = 0.0019$]. Here, we found plants grown in field
257 environments had a significantly greater absolute concentrations of *n*-alkanes (1695 ±
258 1214 μg g^{-1}) compared to the plants grown in enclosed environments, under potentially
259 more controlled conditions (976 ± 432 μg g^{-1}) (**Table 2**).
260
261 Most research on chain-length distributions and concentrations of *n*-alkanes has been
262 undertaken on hydrocarbons extracted from leaf material as leaf waxes are thought to be
263 a major contributor to the organic fraction in geologic sediments. A recent meta-analysis
264 of *n*-alkane concentrations of leaf material from 282 angiosperm species found on
265 average angiosperms had an absolute *n*-alkane abundance of 506 ± 497 μg g^{-1} [43]. Here,
266 we found inflorescences of a single angiosperm, *Cannabis sp.*, had nearly triple the
267 absolute amount of *n*-alkanes compared to angiosperm leaf material. Several studies have
268 noted that inflorescences have greater absolute abundances of *n*-alkanes compared to
269 leaves on the same plant [44-46]. The reasons behind these differences in concentration
270 of *n*-alkanes between floral structures and leaves are unresolved. Inflorescence vigor is
271 critical to reproductive success, and thus the increased lipid concentrations may be a
272 response to provide increased protection of these organs. Waxes on leaf cuticle are
273 considered a strategy to guard against water loss and pathogens [36, 47, 48]. Lipids on
274 the inflorescences may also prevent desiccation of floral components, in addition to

275 acting as a safeguard against microbial or fungal attack or possibly to stabilize other
276 defensive compounds on the inflorescence.
277
278 In addition, we found *Cannabis* plants grown under field conditions had nearly double
279 the absolute concentration of *n*-alkanes on the inflorescences compared to plants grown
280 in enclosed environments (**Table 2**). Previous research has shown that the concentrations
281 of *n*-alkanes and other leaf lipids are affected by the plant's environment (Riederer and
282 Schneider, 1990, Shepard and Griffith, 2006, Bondada et al. 1996). In particular, plants
283 grown in field environments have been shown to produce a greater absolute abundance of
284 *n*-alkanes than their greenhouse-grown counterparts (Shepard et al., 1995). Increased
285 irradiance and UV-B light has been shown to increase the abundance of *n*-alkanes in
286 some species (Gonzolez et al., 1996), decrease the amount of *n*-alkane in other species
287 (Barnes et al., 1996), or cause no change in *n*-alkane absolute amounts (Baker, 1974).
288 Some of the largest differences in the absolute amount of *n*-alkanes have been shown in
289 plants grown under water-stressed or polluted condition (Percy et al., 2002; Dixon et al.,
290 1997; Bondada et al., 1996). While the process behind the difference in *n*-alkane absolute
291 abundance between plants grown in enclosed versus field environments cannot be
292 specifically known in this study, a possible mechanism behind these distribution and
293 concentration patterns may derive from changes in the activity or specificity of particular
294 enzymes involved in fatty acid synthesis, chain elongation, and decarboxylation
295 processes (Shepard and Griffith, 2006). Although the specific mechanism cannot be
296 isolated in our current study, our data from *Cannabis* inflorescences grown in different
297 setting are consistent with these models and suggest a common production mechanism

between leaf and inflorescence waxes.

We compiled peak areas of all *n*-alkanes present in the inflorescence of *Cannabis sp.* to quantify variations in the chain-length distribution of *n*-alkanes using carbon preference indices (CPI) (**Table 1**). Strong odd-over-even predominance of *n*-alkanes is a hallmark of higher plant wax distributions [36, 49, 50] and the distribution of *n*-alkanes in *Cannabis sp*. inflorescences is consistent with these previous observations of leaf waxes (**Table 1**). We found *Cannabis sp*. had an average CPI of 13.6 ± 1.9. In addition, we found significant differences between the growth settings [Welch *t*-test, $t(59.9) = 3.662$, $p = 0.0005$], where the plants grown in field environments had a larger CPI (14.0 ± 2.0) compared to the plants grown in enclosed environments (12.6 ± 1.3) (**Table 2**). The average chain length (ACL) of *Cannabis sp*. *n*-alkanes for all growth settings was 28.8 ± 0.2. However, significant differences between the growth settings was observed [Wilcoxon/Kruskal-Wallis, $W(69.9) = -4.931$, $z = 4.062$, $p < 0.0001$], where the plants grown in open field environments had a smaller ACL (28.8 ± 0.2) compared to the plants grown in enclosed environments (29.0 ± 0.1) (**Table 2**).

Here, we observed *Cannabis* plants grown under field conditions had, on average, greater concentrations of *n*-alkanes with shorter chain lengths and a more pronounced odd-over-even character as compared to plants grown within enclosed systems (**Table 2**). These differences in *n*-alkane distributions and concentrations are possibly related to one or several specific growing conditions not quantified in this study. When contrasting *Cannabis sp.* cultivated in field versus enclosed environments, we would expect field

grown plants to be exposed to a lower average growth temperature (i.e., subject to daily temperature fluctuations) while also exposed to increased water stress and increased irradiance. While limited research has been conducted on inflorescence waxes, previous studies on leaf waxes may provide some explanations for these wax distributions and abundances.

The chain-length distribution of *n*-alkanes on leaves has been linked to various environmental parameters, due to the functionality of waxes in controlling water loss [51]. Recent studies of woody tree species have shown relationships between leaf wax chain-length distributions and growth temperature, in which higher growth temperatures were correlated with increased abundances of longer *n*-alkane chain lengths (e.g., ACL) [41, 52, 53]. ACL values in forbs, grasses, shrubs, and trees have also been shown to vary with aridity, suggesting that plant water relations may additionally influence chain-length distributions [46, 54-59]. In addition to elevated growth temperature and lower water stress, plants cultivated in enclosed environments likely were grown using managed light systems with lower irradiance. It is well established that fatty acid synthesis is strongly connected to illumination levels, as the pathway requires both ATP and NADPH from the light reactions (Sauer and Heise, 1983, Sasaki et al., 1997). Further, Shepard et al. (1995, 1997) showed that irradiance levels affected lipid production, with plants grown under high-light natural environments producing leaf waxes with shorter chain lengths. While limited research has been carried out on inflorescence lipids, our data are consistent with these factors, as it would be expected that *Cannabis* plants cultivated in field environments would be exposed to a decreased average growth temperature, increased

water stress, and increased irradiance. These hypothesized drivers of variations in inflorescence lipid concentrations and distribution could be more fully evaluated through multi-factor growth chamber experiments, which are beyond the scope of this study.

3.2 Carbon isotopes of n-alkanes from Cannabis inflorescences

As *n*-C_{29} was the most abundant *n*-alkane homologue extracted from *Cannabis sp*. inflorescences, we report $\delta^{13}C$ values of *n*-C_{29} ($\delta^{13}C_{n\text{-}C29}$) exclusively. We found the $\delta^{13}C_{n\text{-}C29}$ values of *Cannabis sp*. inflorescences ranged between −56.9 ‰ and −28.9 ‰, with an average $\delta^{13}C_{n\text{-}C29}$ value of −37.3 ± 4.4 ‰ (n = 72, **Table 1**). A significant difference in $\delta^{13}C$ values occurred between plants grown in enclosed environments versus open field conditions [Welch t-test, $t(14.2) = 2.387$, $p = 0.031$]. Here the plants cultivated in open field environments had more positive $\delta^{13}C_{n\text{-alkane}}$ values (−36.2 ± 1.5 ‰) compared to the plants cultivated in enclosed environments (−41.3 ± 8.2 ‰) (**Table 2**).

The large variability in $\delta^{13}C_{n\text{-}C29}$ values from plants grown in enclosed environments is most likely due to variations in the $\delta^{13}C$ values of the source CO_2 available to plants during growth. CO_2 within enclosed settings tends be more depleted in ^{13}C compared to well mixed, outdoor settings for two reasons. First, the lack of sufficient air circulation results in the build up of plant-respired CO_2, which is ^{13}C depleted relative to the ambient air. Second, to elevate plant growth, horticulturalists and agronomists tend to raise CO_2 levels within indoor growth environments through the addition of CO_2. Commercial supplemental CO_2 is most often fossil fuel- or biogenic-derived. Bottled CO_2 from either fossil fuels or biogenic processes typically has much lower $\delta^{13}C$ values compared to

global atmospheric CO_2, resulting in indoor grown plants with extremely low $\delta^{13}C$ values (Farquhar et al., 1989). The lowest $\delta^{13}C_{n\text{-}C29}$ values observed in this dataset were between −60 ‰ and −50 ‰ (**Figure 1**) and would correspond to a source CO_2 with a $\delta^{13}C$ value of approximately −35 ‰ to −25 ‰ [60], equivalent to fossil fuel-derived CO_2 with a $\delta^{13}C$ value of −37 ‰ to −28 ‰ [61, 62]. However, *Cannabis* plants grown in enclosed environments within a well-ventilated atmosphere that allows mixing of CO_2 with the external atmosphere can produce $\delta^{13}C$ values similar to plants grown in open settings. This may explain why the majority of indoor-grown plants have $\delta^{13}C_{n\text{-}C29}$ values similar to the $\delta^{13}C_{n\text{-}C29}$ values of plants grown under open field conditions (**Figure 1**).

We note that a single *Cannabis sp.* inflorescence sample from a plant assigned as having been cultivated within an enclosed environment had a $\delta^{13}C_{n\text{-}C29}$ value of −28.9 ‰, more positive relative to the $\delta^{13}C_{n\text{-}C29}$ values of plants grown in open field environments (**Figure 1**). There are two potential explanations for this very positive $\delta^{13}C_{n\text{-}C29}$ value. First, this plant was possibly grown in a field setting but incorrectly assigned as indoor grown in the DEA records during confiscation and eradication. A second possibility is this plant was grown in bottled CO_2 that had been derived from volcanic or geothermal sources [63].

3.3 Apparent fractionation between inflorescence n-alkanes and bulk Cannabis inflorescences

The $\delta^{13}C$ value of bulk inflorescence ($\delta^{13}C_{Bulk}$) linearly correlated with the $\delta^{13}C_{n\text{-}C29}$ value collected from the same sample (**Figure 2**). A total least squares regression line fitted to the paired data was described by the equation:

$$\delta^{13}C_{n\text{-}C29} = 0.95\times\delta^{13}C_{Bulk} - 9.6\ ‰\ (r^2 = 0.94, F_{1, 71} = 1149.2, p < 0.0001), \quad \textbf{Equation 5}.$$

The slope was not different than 1 at $\alpha = 0.01$. Total least squares regression lines fitted to the paired data separated by enclosed versus open growth settings was described by the equations:

Enclosed: $\delta^{13}C_{n\text{-}C29} = 1.0\times\delta^{13}C_{Bulk} - 7.2\ ‰\ (r^2 = 0.99, F_{1, 14} = 1304.4, p < 0.0001)$, **Equation 6**, and

Open: $\delta^{13}C_{n\text{-}C29} = 0.90\times\delta^{13}C_{Bulk} - 11.1\ ‰\ (r^2 = 0.50, F_{1, 56} = 55.1, p < 0.0001)$, **Equation 7**, respectively.

When compared, we found the slopes for $\delta^{13}C_{n\text{-}C29}$ values versus $\delta^{13}C_{Bulk}$ for the two growth settings were not different ($p > 0.01$) from one another (**Figure 2**). However, the intercepts for these regressions were different and thus, cannot be described by a single slope and intercept, possibly suggesting different behaviors between the two growth settings.

We found the apparent fractionation (ε_{app}) between *n*-C_{29} extracted from *Cannabis sp*. inflorescence and bulk *Cannabis sp*. inflorescence materials ranged between −11.3 ‰ and −4.8 ‰ in individual samples, with an average of −8.0 ± 1.1 ‰ (n = 72, **Table 1**). A significant difference was found between the plants grown within an enclosed system versus those grown in field environments [Welch t-test, $t(27.0) = 3.869$, $p = 0.0006$], where the plants grown in enclosed environments had a more positive ε_{app} value (−7.3 ± 0.8 ‰, n = 15) compared to the plants grown in open field environments (−8.2 ± 1.0 ‰, n = 57) (**Table 2**).

Considering the distinction in absolute abundance of *n*-alkanes between the plants grown under the two growth settings, an apparent difference in fractionation may not be unexpected. Bulk isotope analysis represents a cumulative measurement of all chemical constituents and tissues, whereas compound-specific isotope analysis explicitly isolates individual components from the bulk material. The compounds of interest to this study are the *n*-alkyl lipids, but *Cannabis sp*. is well known for producing a wide variety of other compounds, particularly terpenoids [27, 30, 32]. The carbon isotopic fractionation during terpenoid biosynthesis has been characterized and the apparent fractionation during biosynthesis, as measured relative to bulk leaf tissue, is significantly less negative than that observed for *n*-alkyl lipids [24, 64]. Considering the bulk isotope measurement represents the analysis of a complex mixture of these compounds, in addition to many others with less understood carbon isotopic signatures and fractionations, it should be expected that the bulk $\delta^{13}C$ value of *Cannabis sp*. might be significantly influenced by variations in the combination of these chemical components. As we do not have direct

433 measurements of source CO_2, we cannot assess if the difference in ε_{app} between *n*-alkanes
434 extracted from *Cannabis sp*. inflorescence and bulk *Cannabis sp*. inflorescence materials
435 for the two growth environments is affected by the environmental conditions or if the
436 difference is due to variation in chemical composition. Nonetheless, these data support
437 the notion that compound-specific isotope measurements provide a more direct measure
438 of plant biochemistry and ecology than bulk isotope measurements.

439

440 *3.4 Potential applications of inflorescence n-alkanes in emerging marijuana markets*

441

442 Stable isotope analyses of marijuana have a demonstrated potential to improve the
443 forensic and law enforcement communities' understanding of marijuana production
444 methods, growth setting, and trafficking networks [1-3]. In this respect, $\delta^{13}C$—as well as
445 nitrogen ($\delta^{15}N$)—isotope values have proven moderately useful. In a series of papers,
446 Shibuya and colleagues demonstrated the potential to differentiate three of the five major
447 production regions of marijuana cultivation in Brazil based on observed differences in the
448 bulk $\delta^{13}C$ and $\delta^{15}N$ isotope values of seized marijuana samples [4, 5]. West and others
449 followed with a study of eradicated and seized material from the U.S., but could not to
450 distinguish region-of-origin based on bulk $\delta^{13}C$ and $\delta^{15}N$ values alone [6]. While growth
451 location could not be assigned in that work, the growth setting could be identified using
452 $\delta^{13}C$ values of bulk materials (e.g., leaves, inflorescence) as plants grown in field
453 environments had unique values compared to plants grown within an enclosed
454 glass/hothouse system [6]. Following on these findings, Hurley et al. (2010a) developed a
455 cultivation model that defined theoretical cut-off limits for $\delta^{13}C_{Bulk}$, where values more

456 negative than −32.0 ‰ were indicative of *Cannabis* plants grown in enclosed
457 environments and values more positive than −29.0 ‰ were plants grown outdoors.
458 Values more positive than −32.0 ‰ and more negative than −29.0 ‰ could either be
459 assigned to plants grown outdoors in shaded conditions or indoors [38]. The authors
460 found in a blind test of their model that 88 % of indoor-grown plants were correctly
461 identified as to growth setting, while 98 % of outdoor-grown plants were correctly
462 assigned [38].
463
464 We tested the application of this cultivation model to $\delta^{13}C_{n\text{-}C29}$ values measured in the
465 current study by converting $\delta^{13}C_{n\text{-}C29}$ values to $\delta^{13}C_{Bulk}$ values using ε_{app} (**Figure 3**).
466 Assignments of plants cultivated in enclosed environments, shaded or enclosed
467 environments, or open field environments were made for all 72 specimens using the
468 average ε_{app} values between *n*-C_{29} and *Cannabis* inflorescences from this study. Here,
469 when the average ε_{app} value between *Cannabis n*-C_{29} and inflorescence is used (−8.0 ‰),
470 we found that 7 plants were assigned to enclosed environments, 20 were assigned to
471 either shaded open environments or enclosed environments, and 45 were assigned to
472 open field environments. In this exercise, 98 % of the *Cannabis* plants cultivated
473 outdoors were correctly identified and 60 % of the plants cultivated in enclosed
474 environments were assigned correctly. These finding indicate that by using the *Cannabis*
475 inflorescence-specific ε_{app} value for calculating $\delta^{13}C_{Bulk}$ values and assigning growth
476 setting, the overall reliability of the model was 90%.
477
478 The $\delta^{13}C$ values presented here for the *n*-C_{29} from inflorescence suggest that the

cultivation environment (e.g., growth setting) could be established with either bulk plant material or compound-specific inflorescence $\delta^{13}C$ values. However, increased reliability may be achieved if inflorescence *n*-alkane concentrations and distributions were included in the model allowing for a growth setting-specific ε_{app} value to be used (**Table 2**). A specific advantage of compound-specific isotope measurements is that bulk tissue is not needed to make an isotopic measurement and these specific compounds may be isolated from complex mixtures such as *Cannabis* extracts and infused products. While stringently controlled growth experiments are needed to determine the specific mechanism(s) behind the findings presented here, this study of plants grown in "real world" settings demonstrates that the carbon isotope ratios and concentrations of *n*-alkanes has the potential to become an ideal regulatory tool to establish growth settings of *Cannabis* materials post-harvest.

4. Conclusions

Here we presented chain-length distributions and concentrations of *n*-alkanes, plus carbon isotope ratios of *n*-C_{29} extracted from *Cannabis sp.* inflorescences. We found chain-length distributions, concentrations, and carbon isotope variations of these lipids relate to growth setting. While the biosynthetic mechanism is unknown, we found that inflorescences of *Cannabis sp.* have nearly 3-times the concentrations of *n*-alkanes than the average angiosperm leaf and that *Cannabis* plants grown under field conditions have significantly more inflorescence *n*-alkanes relative to plants grown within enclosed environments. Carbon isotope ratios of *Cannabis sp.* inflorescences largely reflect the

isotope composition of source CO_2, which can vary greatly in enclosed environments. In addition, we found that *n*-alkanes from *Cannabis* plants grown within enclosed environments had a large range of $\delta^{13}C$ values with both the most positive and most negative $\delta^{13}C$ values in this dataset reported.

Together, these findings suggest that inflorescence lipid distributions, concentrations, and carbon isotope values have the potential to be used to identify the growth setting of *Cannabis sp.* plants. As legal and illegal commercial production of marijuana increases, the need to establish the growth setting of *Cannabis* will also increase. Many communities, municipalities, and jurisdictions in the U.S. where *Cannabis* production is legal now regulate how the product is grown. With additional jurisdictions seeking to legalize marijuana usage for both medical and recreational purposes, state and federal regulators will need additional analytical tools to certify a *Cannabis* products cultivation setting. In this study, we show that distributions, concentrations, and carbon isotopic variations in specific inflorescence lipids are related to growth setting and suggest that this tool may potentially be useful to support or refute a producer's claim regarding the growth setting of *Cannabis*.

References:

[1] Liu JH, Lin WF, Fitzgerald MP, Saxena SC, Shieh YN. Possible characterization of samples of *Cannabis sativa* L. by their carbon isotopic distributions. Journal of Forensic Science. 1979;24:814-6.

[2] Denton TM, Schmidt S, Critchley C, Stewart GR. Natural abundance of stable carbon and nitrogen isotopes in *Cannabis sativa* reflect growth conditions. Australian Journal of Plant Physiology. 2001;28:1005-12.
[3] Galimov EM, Sevastyanov VS, Kulbachevskaya EV, Golyavin AA. Isotope ratio mass spectrometry: $\delta^{13}C$ and $\delta^{15}N$ analysis for tracing the origin of illicit drugs. Rapid Communications in Mass Spectrometry. 2005;19:1213-6.
[4] Shibuya EK, Sarkis JES, Negrini-Neto O, Martinelli LA. Carbon and nitrogen stable isotopes as indicative of geographical origin of marijuana samples seized in the city of San Paulo, Brazil. Forensic Science International. 2007;167:8-15.
[5] Shibuya EK, Sarkis JES, Negrini-Neto O, Moreira MZ, Victoria RL. Sourcing Brazilian marijuana by applying IRMS analysis to seized samples. Forensic Science International. 2006;160:35-43.
[6] West JB, Hurley JM, Ehleringer JR. Stable Isotope Ratios of Marijuana. I. Carbon and Nitrogen Stable Isotopes Describe Growth Conditions*. Journal of Forensic Sciences. 2009;54:84-9.
[7] Farquhar GD, Ehleringer JR, Hubick KT. Carbon isotope discrimination and photosynthesis. Annual Review of Plant Physiology and Molecular Biology. 1989;40:503-37.
[8] O'Leary MN. Carbon isotope fractionation in plants. Phytochemistry. 1981;20:553-67.
[9] Beerling DJ, Heath J, Woodward FI, Mansfield TA. Drought-CO_2 Interactions in Trees: Observations and Mechanisms. New Phytologist. 1996;134:235-42.
[10] Ehleringer JR. Correlations between carbon isotope discrimination and leaf conductance to water vapor in common beans. Plant Physiology. 1990;93:1422-5.
[11] Ehleringer JR, Cerling TE. Atmospheric CO_2 and the Ratio of Intercellular to Ambient CO_2 Concentrations in Plants. Tree Physiology. 1995;15:105-11.
[12] Farquhar GD, Ball MC, von Caemmerer S, Roksandic Z. Effect of Salinity and Humidity on $\delta^{13}C$ Value of Halophytes- Evidence for Diffusional Isotope Fractionation Determined by the Ratio of Intercellular-Atmospheric Partial Pressure of CO_2 Under Different Environmental Conditions Oecologia. 1982;52:121-4.
[13] Farquhar GD, Schulze ED, Kuppers M. Responses to humidity by stomata of *Nicotiana glauca* L. and *Corylus avellana* L. are consistent with the optimization of carbon dioxide uptake with respect to water loss. Australian Journal of Plant Physiology. 1980;7:315-27.
[14] Farquhar GD, Sharkey TA. Stomatal conductance and photosynthesis. Annual Review of Plant Physiology and Molecular Biology. 1982;33:317-45.
[15] Panek JA, Waring RH. Carbon isotope variation in Douglas-fir foliage: improving the $\delta^{13}C$-climate relationship. Tree Physiology. 1995;15:657-63.
[16] Sparks JP, Ehleringer JR. Leaf carbon isotope discrimination and nitrogen content for riparian trees along elevational transects. Oecologia. 1997;109:362-7.
[17] Winter K, Holtum JAM, Edwards GE, O'Leary MH. Effect of low relative humidity on $\delta^{13}C$ value in two C_3 grasses and in Panicum milioides, a C_3-C_4 intermediate species. Journal of Experimental Botany. 1982;33:88-91.
[18] Zimmerman J, Ehleringer JR. Carbon isotope ratios are correlated with irradiance levels in the Panamanian orchid *Catasetum viridiflavum*. Oecologia. 1990;83:247-9.

[19] Ehleringer JR, Field CB, Lin ZF, Kuo CY. Leaf carbon isotope and mineral composition in subtropical plants along an irradiance cline. Oecologia. 1986;70:520-6.
[20] Smith BN, Oliver J, McMillan C. Influence of carbon source, oxygen concentration, light intensity, and temperature on C^{13}/C^{12} ratios in plant tissues. Botany Gazette. 1976;137:99-104.
[21] Yang H, Pagani M, Briggs DEG, Equiza MA, Jagels R, Leng Q, et al. Carbon and hydrogen isotope fractionation under continuous light: implications for paleoenvironmental interpretations of the High Arctic during Paleogene warming. Oecologia. 2009;160:461-70.
[22] Pearcy RW, Pfitsch WA. Influence of sunflecks on the ^{13}C of *Adenocaulon bicolor* plants occurring in contrasting forest understory microsites. Oecologia. 1991;86:457-62.
[23] Pedentchouk N, Sumner W, Tipple BJ, Pagani M. $\delta^{13}C$ and δD compositions of n-alkanes from modern angiosperms and conifers: An experimental set up in central Washington State, USA. Organic Geochemistry. 2008;39:1066-71.
[24] Diefendorf AF, Freeman KH, Wing SL, Graham HV. Production of *n*-alkyl lipids in living plants and implications for the geologic past. Geochimica et Cosmochimica Acta. 2011;75:7472-85.
[25] Diefendorf AF, Mueller KE, Wing SL, Koch PL, Freeman KH. Global patterns in leaf ^{13}C discrimination and implications for studies of past and future climate. Proceedings of the National Academy of Science. 2010;107:5738-43.
[26] Tipparat P, Kunkaew W, Julsrigival S, Pinmanee S, Natakankitkul S. Classification of Cannabis Plants Grown in Northern Thailand using Physico-Chemical Properties. Journal of Natural Sciences Research. 2014;4:46-54.
[27] ElSohly MA, Ross SA, Mehmedic Z, Arafat R, Yi B, Banahan III BF. Potency trends of Δ^9-THC and other cannabinoids in confiscated marijuana from 1980-1997. Journal of Forensic Science. 2000;45:24-30.
[28] Chandra S, Lata H, Mehmedic Z, Khan IA, ElSohly MA. Assessment of Cannabinoids content in micropropagated plants of *Cannabis sativa* and their comparison with conventionally propagated plants and mother plants during developmental stages of growth. Planta Medica. 2010;76:743-50.
[29] Ilias Y, Rudaz S, Mathieu P, Christen P, Veuthey JL. Extraction and analysis of different cannabis samples by headspace solid-phase microextraction combined with gas chromatography-mass spectometry. Journal of Separation Science. 2005;28:2293-300.
[30] Fischedick JT, Hazekamp A, Erkelens T, Choi YH, Verpoorte R. Metabolic fingerprinting of *Cannabis sativa* L., cannabinoids and terpenoids for chemotaxonomic and drug standardization purposes. Phytochemistry. 2010;71:2058-73.
[31] Muccio Z, Wockel C, An Y, Jackson GP. Comparison of bulk and compound-specific $\delta^{13}C$ isotope ratio analysis for the discrimination between Cannabis samples. Journal of Forensic Science. 2011;57:757-64.
[32] Latta RP, Eaton BJ. Seasonal fluctuations in cannabinoid content of Kansas Marijuana. Economic Botany. 1975;29:153-63.
[33] Barni-Comparini I, Ferri S, Centini F. Cannabinoid level in the leaves as a tool for the early discrimination of cannabis chemovariants. Forensic Science International. 1984;24:37-42.
[34] Mechtler K, Bailer J, de Hueber K. Variations in the Δ^9-THC content in single plant of hemp varieties. Industrial Crops and Products. 2004;19:19-24.

618 [35] Burgdorf JR, Kilmer B, Pacula RL. Heterogeneity in the composition of marijuana
619 seized in California. Drug and Alcohol Dependence. 2011;117:59-61.
620 [36] Eglinton G, Hamilton RJ. Leaf Epicuticular Waxes. Science. 1967;156:1322-35.
621 [37] Schimmelmann A, Sessions AL, Mastalerz M. Hydrogen Isotopic (D/H)
622 Composition of Organic Matter During Diagenesis and Thermal Maturation. Annual
623 Review of Earth and Planetary Sciences. 2006;34:501-33.
624 [38] Hurley JM, West JB, Ehleringer JR. Stable isotope models to predict geographic
625 origin and cultivation conditions of marijuana. Science and Justice. 2010;50:86-93.
626 [39] West JB, Hurley JM, Dudas FO, Ehleringer JR. The Stable Isotope Ratios of
627 Marijuana. II. Strontium Isotopes Relate to Geographic Origin. Journal of Forensic
628 Sciences. 2009;54:1261-9.
629 [40] Hurley JM, West JB, Ehleringer JR. Tracing retail cannabis in the United States:
630 Geographic origin and cultivation patterns. International Journal of Drug Policy.
631 2010;21:222-8.
632 [41] Tipple BJ, Pagani M. Environmental control on eastern broadleaf forest species' leaf
633 wax distributions and D/H ratios. Geochimica et Cosmochimica Acta. 2013;111:64-77.
634 [42] Marzi R, Torkelson BE, Olson RK. A revised carbon preference index. Organic
635 Geochemistry. 1993;20:1303-6.
636 [43] Bush RT, McInerney FA. Leaf wax *n*-alkane distributions in and across modern
637 plants: Implications for paleoecology and chemotaxonomy. Geochimica et
638 Cosmochimica Acta. 2013;117:161-79.
639 [44] Shu B, Lin L, Zhang Y, Wang H, Luo H. *N*-alkane profiles of common rangeland
640 species in northern China and the influence of drying method on their concentrations.
641 Canadian Journal of Plant Science. 2008;88:137-41.
642 [45] Gamarra B, Kahmen A. Concentrations and δ^2H values of cuticular n□alkanes vary
643 significantly among plant organs, species and habitats in grasses from an alpine and a
644 temperate European grassland. Oecologia. 2015.
645 [46] Rommerskirchen F, Plader A, Eglinton G, Chikaraishi Y, Rullkotter J.
646 Chemotaxonomic significance of distribution and stable carbon isotopic composition of
647 long-chain alkanes and alkan-1-ols in C_4 grass waxes. Organic Geochemistry.
648 2006;37:1303-32.
649 [47] Riederer M, Markstadter C. Cuticular waxes: a critical assessment of current
650 knowledge. In: Kersteins G, editor. Plant cuticles: an integrated functional approach.
651 Oxford: BIOS Scientific Publishers; 1996. p. 189-200.
652 [48] Guiz PG. Epicuticular leaf waxes in the evolution of the plant kingdom. Journal of
653 Plant Physiology. 1994;143:453-64.
654 [49] Lockheart MJ, Van Bergen PF, Evershed RP. Variation in the stable carbon isotope
655 composition of individual lipids from the leaves of modern angiosperms: implications for
656 the study of higher land plant-derived sedimentary organic matter. Organic
657 Geochemistry. 1997;26:137-53.
658 [50] Piasentier E, Bovolenta S, Malossini F. The *n*-alkane concentrations in buds and
659 leaves of browsed broadleaf trees. Journal of Agricultural Science. 2000;135:311-20.
660 [51] Shepherd T, Griffiths DW. The effects of stress on plant cuticular waxes. New
661 Phytologist. 2006;171:469-99.

[52] Sachse D, Radke J, Gleixner G. δD values of individual *n*-alkanes from terrestrial plants along a climatic gradient – Implications for the sedimentary biomarker record. Organic Geochemistry. 2006;37:469-83.
[53] Riederer M, Schneider G. The effect of the environment on the permeability and composition of *Citrus* leaf cuticle. Planta. 1990;180:154-65.
[54] Hughen KA, Eglinton TI, Xu L, Makou M. Abrupt tropical vegetation response to rapid climate changes. Science. 2004;304:1955-9.
[55] Schefuss E, Ratmeyer V, Stuut JBW, Jansen JHF, Sinninghe Damste JS. Carbon isotope analyses of *n*-alkanes in dust from the lower atmosphere over the central eastern Atlantic. Geochimica et Cosmochimica Acta. 2003;67:1757-67.
[56] Rommerskirchen F, Eglinton G, Dupont L, Guntner U, Wenzel C, Rullkotter J. A north to south transect of Holocene southeast Atlantic continental margin sediments: Relationship between aerosol transport and compound-specific $\delta^{13}C$ land plant biomarker and pollen records. Geochemistry Geophysics Geosystems. 2003;4:1101.
[57] Vogts A, Moossen H, Rommerskirchen F, Rullkotter J. Distribution patterns and stable carbon isotopic composition of alkanes and alkan-1-ols from plant waxes of African rain forest and savanna C_3 species. Organic Geochemistry. 2009;40:1037-54.
[58] Vogts A, Schefuss E, Badewien T, Rullkotter J. *n*-Alkane parameters from a deep sea sediment transect off southwest Africa reflect continental vegetation and climate conditions. Organic Geochemistry. 2012;47:109-19.
[59] Shepherd T, Robertson GW, Griffiths DW, Birch ANE, Duncan G. Effects of environment on the composition of epicuticular wax from kale and swede. Phytochemistry. 1995;40:407-17.
[60] Tipple BJ, Pagani M. A 35 Myr North American Leaf-Wax Compound-Specific Carbon and Hydrogen Isotope Record: Implications for C_4 Grasslands and Hydrologic Cycle Dynamics. Earth and Planetary Science Letters. 2010;299:250-62.
[61] Pataki DE, Bush SE, Ehleringer JR. Stable isotopes as a tool in urban ecology. In: Flanagan LB, Ehleringer JR, Pataki DE, editors. Stable Isotopes and Biosphere - Atmosphere Interactions: Processes and Biological Controls: Academic Press; 2005. p. 400.
[62] Pataki DE, Xu T, Luo YQ, Ehleringer JR. Inferring biogenic and anthropogenic CO_2 sources across an urban to rural gradient. Oecologia. 2007;152:307-22.
[63] Deines P. The isotopic composition of reduced organic carbon. In: Fritz P, Fontes JC, editors. Handbook of Environmental Isotope Geochemistry: I The Terrestrial Environment. Amsterdam: Elsevier; 1980. p. 329-406.
[64] Diefendorf AF, Freeman KH, Wing SL. Distribution and carbon isotope patterns of diterpenoids and triterpenoids in modern temperate C_3 trees and their geochemical significance. Geochimica et Cosmochimica Acta. 2012;85:342-56.

Highlights:

Cultivation setting relates to the distribution and amount of *n*-alkanes.

$\delta^{13}C$ values of CO_2 of the growth environment controlled the $\delta^{13}C$ values of *n*-C_{29}.

Cannabis cultivated in enclosed environments had significantly lower $\delta^{13}C$ values.

The correct growth environment was assigned 90 % of time from $\delta^{13}C$ values of *n*-C_{29}.

Inflorescence *n*-alkanes may be used to trace the cultivation method of *Cannabis*.

Acknowledgements

Mahmoud ElSohly and Zlatko Mehmedic at the University of Mississippi provided *Cannabis* specimens and collection information. B.J.T. and J.R.E. designed experiment. B.H. and J.E.B. performed extractions and purifications and provided intellectual input and contributed to the text. B.J.T. and B.H. carried out concentration and compound-specific isotope analysis. L.A.C and J.R.E. provided intellectual input, support, and contributed to the text. B.J.T. was the lead in writing this work. This contribution was strengthened by comments from two anonymous reviewers. This research was supported by NSF-ISO-1052551 awarded to J.R.E. and B.J.T.

722 **Figures**

723 **Figure 1**

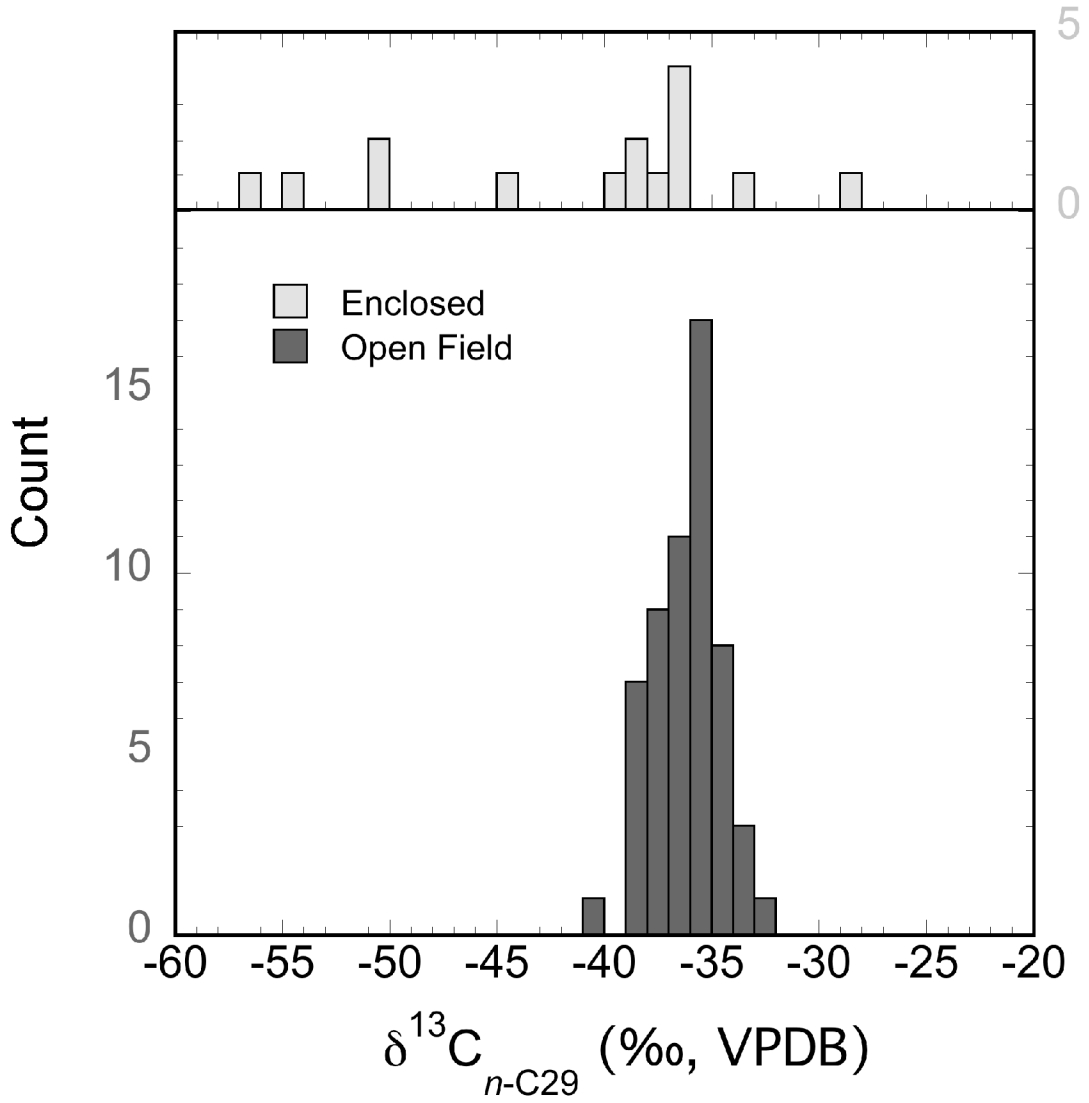

724

725 **Figure 1. A.** Histograms of carbon isotope ratios of *n*-C_{29} extracted from domestic
726 *Cannabis sp.* inflorescences grown within enclosed environments (light grey) and field
727 conditions (dark grey).
728

729

729
730 **Figure 2**
731
732
733

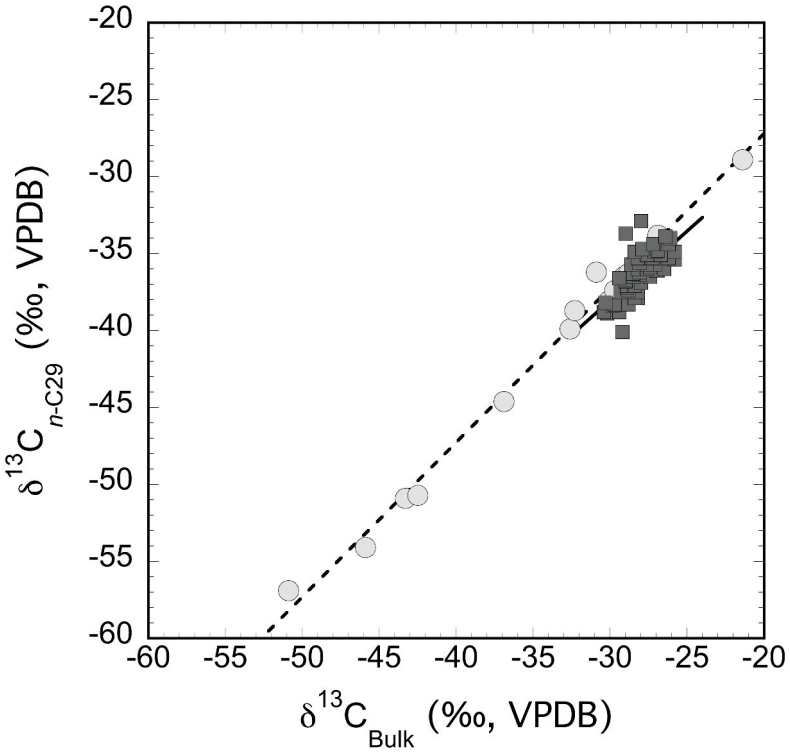

734
735
736
737 **Figure 2.** Cross-plot of the carbon isotope values ($\delta^{13}C$) of *n*-C_{29} extracted from
738 inflorescences *versus* bulk inflorescence materials. The hashed and solid lines indicate
739 regressions for plants grown within enclosed and field environments, respectively. The
740 regressions for plants grown within enclosed and field environments are $\delta^{13}C_{n\text{-}C29} =$
741 $1.0\times\delta^{13}C_{Bulk} - 7.2‰$ and $\delta^{13}C_{n\text{-}C29} = 0.90\times\delta^{13}C_{Bulk} - 11.1‰$, respectively.
742
743

743 **Tables.**
744

Table 1. Concentrations, distributions, and carbon isotope values of *n*-alkanes from Cannabis inflorescence

ID	Cultivation Setting	State	*n*-C_{23} (µg/g)	*n*-C_{24} (µg/g)	*n*-C_{25} (µg/g)	*n*-C_{26} (µg/g)	*n*-C_{27} (µg/g)	*n*-C_{28} (µg/g)	*n*-C_{29} (µg/g)	*n*-C_{30} (µg/g)	*n*-C_{31} (µg/g)	*n*-C_{32} (µg/g)	*n*-C_{33} (µg/g)	ACL	CPI	*n*-C_{29} $\delta^{13}C$ (‰, VPDB)	SD	Bulk[#] $\delta^{13}C$ (‰, VPDB)	ε_{app} (‰, VPDB)
784	Open-Field	AK	1	1	5	138	31	565	23	100	0	0		28.8	13.7	-35.3	0.1	-27.5	-8.0
786	Enclosed	AK	1	1	11	374	68	1183	36	239	7	8		28.9	13.2	-37.4	0.0	-29.7	-8.0
787	Enclosed	AK	1	1	5	92	29	506	29	124	1	3		29.0	11.3	-36.9	1.2	-30.9	-6.4
430	Enclosed	CA	1	1	6	128	34	670	29	123	2	6		28.9	13.2	-28.9	0.3	-21.4	-7.6
708	Enclosed	CA	2	1	7	140	30	507	26	95	1	0		28.8	11.8	-36.5	0.5	-29.1	-7.6
761	Open-Field	CA	1	1	7	254	62	1122	54	203	4	3		28.9	12.4	-35.3	0.1	-28.2	-7.3
762	Open-Field	CA	0	1	3	75	16	449	14	64	0	0		28.9	17.6	-34.4	0.2	-26.2	-8.4
763	Open-Field	CA	0	0	2	169	39	1155	42	185	4	4		29.0	17.5	-	-	-	-
780	Open-Field	CA	1	1	9	239	67	1340	64	241	1	1		28.9	13.0	-35.1	0.2	-26.7	-8.6
781	Open-Field	CA	2	1	9	271	82	1249	56	164	0	0		28.8	11.5	-33.9	0.1	-26.4	-7.7
658	Enclosed	FL	3	2	4	75	35	1054	49	241	4	1		29.2	14.7	-	-	-	-
308	Open-Field	HI	2	1	11	152	60	1310	69	194	4	6		29.0	11.6	-36.6	0.1	-29.4	-7.3
502	Open-Field	HI	2	2	18	385	108	1958	87	298	6	5		28.9	12.2	-35.6	1.2	-28.1	-7.5
663	Open-Field	HI	2	1	18	392	73	1516	54	211	4	8		28.8	14.4	-36.8	0.0	-29.0	-8.0
664	Enclosed	HI	1	1	7	149	45	990	47	211	1	0		29.0	13.7	-	-	-	-
667	Open-Field	HI	1	1	7	115	49	1084	64	220	5	4		29.1	11.8	-36.2	0.2	-28.1	-8.3
668	Open-Field	HI	0	0	4	51	13	198	13	63	3	2		29.0	9.5	-37.1	0.1	-28.9	-8.4
669	Open-Field	HI	1	0	2	73	15	244	12	60	1	2		28.9	12.4	-36.0	0.0	-28.2	-8.0
670	Open-Field	HI	3	2	20	388	34	421	18	64	2	2		27.9	13.1	-38.3	0.2	-29.7	-8.9
676	Open-Field	HI	1	1	7	160	43	633	28	103	3	2		28.8	11.1	-35.7	0.3	-28.6	-7.4
710	Open-Field	HI	2	0	7	258	61	1456	59	216	0	0		28.9	15.4	-35.7	0.3	-27.1	-8.8
712	Enclosed	HI	1	1	5	52	18	372	21	79	0	0		29.0	10.9	-33.8	0.3	-26.9	-7.1
753	Open-Field	HI	1	1	8	261	39	821	37	246	4	2		28.9	15.3	-34.9	0.0	-27.1	-8.0
754	Open-Field	IL	1	1	8	239	36	682	30	204	5	7		28.8	14.5	-	-	-	-
428	Open-Field	IN	1	1	6	154	45	1155	34	155	0	0		28.9	17.1	-35.4	0.0	-25.8	-9.9
264	Open-Field	IN	1	1	4	87	19	421	14	76	6	0		28.9	13.6	-38.4	0.3	-29.8	-9.0
288	Enclosed	IN	1	1	3	85	26	437	19	87	1	2		29.0	12.3	-38.1	0.2	-30.1	-8.2
302	Enclosed	IN	1	1	5	132	55	1184	37	246	4	7		29.1	12.9	-36.2	0.1	-30.9	-5.4
343	Enclosed	IN	1	1	3	87	26	552	29	129	2	3		29.1	12.8	-34.1	0.1	-25.9	-8.6
349	Open-Field	IN	0	1	3	66	17	436	14	78	1	0		29.0	17.3	-34.9	0.0	-25.8	-9.4
363	Open-Field	IN	0	1	8	205	26	484	14	66	1	2		28.5	15.4	-37.5	1.8	-28.2	-9.6
379	Open-Field	IN	1	1	8	178	34	581	25	98	0	0		28.7	12.9	-34.0	0.2	-26.1	-8.1
483	Open-Field	IN	2	1	20	698	91	1590	58	329	7	8		28.6	15.1	-36.9	0.9	-28.0	-9.1
501	Open-Field	IN	2	1	31	127	21	265	11	32	0	0		28.3	11.4	-38.8	0.2	-29.4	-9.7
513	Enclosed	IN	1	1	24	205	40	869	37	146	3	4		28.8	12.5	-36.6	0.1	-29.2	-7.6
514	Open-Field	IN	3	1	10	316	97	2477	139	487	10	10		29.0	12.7	-36.0	0.0	-28.1	-8.2
532	Open-Field	IN	2	2	14	316	41	649	24	127	2	3		28.5	14.1	-35.7	0.0	-27.6	-8.3
534	Open-Field	IN	1	1	7	242	36	656	29	195	4	4		28.8	15.0	-38.3	0.4	-28.8	-9.7
536	Open-Field	IN	2	1	13	321	49	796	28	114	2	3		28.5	13.9	-37.2	0.2	-28.9	-8.6
542	Open-Field	IN	1	1	9	316	76	1558	67	321	5	9		28.9	14.3	-36.4	0.1	-28.1	-8.5
548	Open-Field	IN	3	2	11	198	30	523	15	63	1	1		28.4	13.9	-35.9	0.2	-27.4	-8.8

[#] As reported in West et al., 2009b.

Table 1. cont. Concentrations, distributions, and carbon isotope values of *n*-alkanes from Cannabis inflorescence

ID	Cultivation Setting	State	n-C_{23} (µg/g)	n-C_{24} (µg/g)	n-C_{25} (µg/g)	n-C_{26} (µg/g)	n-C_{27} (µg/g)	n-C_{28} (µg/g)	n-C_{29} (µg/g)	n-C_{30} (µg/g)	n-C_{31} (µg/g)	n-C_{32} (µg/g)	n-C_{33} (µg/g)	CPI	ACL	n-C_{29} $\delta^{13}C$ (‰, VPDB)	SD	Bulk# $\delta^{13}C$ (‰, VPDB)	ε_{app} (‰, VPDB)
682	Open-Field	KY	2	1	49	16	504	82	1321	73	328	9	10	12.2	28.8	-35.3	0.3	-27.2	-8.4
683	Open-Field	KY	1	1	8	3	78	25	405	17	62	0	0	12.0	28.9	-37.5	0.0	-28.5	-9.3
700	Open-Field	KY	2	2	40	13	394	69	1068	49	269	0	0	13.3	28.8	-36.5	0.3	-27.4	-9.3
434	Open-Field	MO	1	0	3	1	33	22	558	62	262	13	9	8.7	29.6	-40.1	0.2	-29.2	-11.3
556	Open-Field	MO	1	1	16	6	205	35	697	24	140	2	3	15.6	28.8	-	-	-	-
557	Open-Field	MO	2	1	34	10	312	44	770	27	117	6	0	14.0	28.6	-36.0	0.1	-27.6	-8.6
558	Open-Field	MO	1	1	15	5	173	46	758	41	143	4	2	11.4	28.9	-	-	-	-
559	Open-Field	MO	13	2	41	12	415	76	1479	65	368	8	12	14.3	28.9	-34.7	0.6	-27.9	-7.1
562	Open-Field	MO	2	1	77	28	605	107	1606	71	362	6	10	12.4	28.7	-34.4	0.1	-27.2	-7.4
565	Open-Field	MO	1	1	22	7	180	27	596	18	94	2	3	16.5	28.7	-36.1	-	-26.9	-9.4
592	Open-Field	MO	36	3	264	36	1296	111	2058	71	410	9	9	17.4	28.3	-38.2	0.1	-30.3	-8.2
279	Enclosed	MT	1	1	8	4	60	22	569	32	152	3	3	12.9	29.2	-50.7	0.1	-42.5	-8.6
792	Enclosed	NY	1	1	19	6	169	37	554	22	103	3	3	12.4	28.8	-	-	-	-
268	Enclosed	OR	1	1	13	4	84	19	320	13	60	1	2	12.7	28.8	-50.9	0.2	-43.3	-7.9
269	Enclosed	OR	0	0	3	1	28	8	176	9	47	1	1	13.2	29.1	-	-	-	-
427	Open-Field	OR	2	1	40	14	393	53	1104	29	139	2	5	17.1	28.6	-36.1	0.0	-27.0	-9.3
493	Open-Field	OR	4	2	109	22	783	93	1957	54	256	2	8	18.0	28.5	-35.7	0.0	-27.4	-8.5
494	Open-Field	OR	2	3	57	10	510	78	1645	79	221	0	0	14.3	28.7	-32.9	0.4	-28.0	-5.0
496	Open-Field	OR	9	2	144	24	1013	201	4859	198	847	16	21	15.6	28.9	-	-	-	-
498	Open-Field	OR	2	2	63	16	465	73	1248	44	254	5	6	14.5	28.7	-34.9	1.3	-28.4	-6.7
525	Open-Field	OR	1	1	38	11	230	42	641	21	68	1	1	12.9	28.5	-37.4	0.1	-28.8	-8.8
570	Open-Field	OR	1	1	40	15	230	36	508	17	48	1	1	11.9	28.4	-37.9	0.3	-28.4	-9.7
571	Open-Field	OR	1	1	20	7	166	34	535	20	91	5	3	12.2	28.7	-36.5	0.3	-28.5	-8.2
598	Open-Field	OR	3	2	103	23	577	78	1425	46	275	4	9	15.7	28.6	-34.8	0.0	-26.9	-8.2
599	Open-Field	OR	2	1	52	12	427	56	1061	36	164	2	4	15.9	28.6	-35.3	0.2	-26.2	-9.3
600	Open-Field	OR	5	3	211	41	1295	148	2887	110	716	15	20	16.2	28.6	-38.8	0.3	-30.4	-8.7
601	Open-Field	OR	1	1	22	9	215	54	884	40	167	4	5	11.9	28.9	-37.5	0.0	-29.3	-8.4
401	Open-Field	TN	1	0	8	2	74	16	437	16	89	3	4	16.0	29.0	-36.3	0.1	-28.5	-7.9
417	Open-Field	TN	1	1	5	2	47	13	275	13	45	0	0	13.0	28.9	-36.7	0.1	-29.0	-7.9
458	Open-Field	TN	2	1	17	7	184	49	1043	36	179	3	3	14.6	28.9	-33.7	1.3	-29.0	-4.8
477	Open-Field	TN	1	1	12	5	96	32	980	45	172	4	5	14.1	29.1	-37.9	0.1	-28.2	-10.0
509	Open-Field	TN	2	2	10	7	80	26	580	23	129	2	4	13.4	29.1	-38.9	0.1	-30.2	-9.0
679	Enclosed	TX	1	0	7	4	78	23	353	22	88	2	2	10.1	29.0	-37.1	0.0	-28.4	-8.9
365	Open-Field	VT	1	1	14	3	60	14	320	10	40	0	2	15.6	28.8	-	-	-	-
704	Enclosed	WA	1	1	12	6	140	41	578	31	111	3	3	10.4	28.9	-	-	-	-
705	Enclosed	WA	1	1	15	6	187	45	829	34	157	1	4	13.6	28.9	-39.9	0.5	-32.6	-7.5
706	Enclosed	WA	2	2	12	6	76	23	460	21	107	0	0	12.3	29.0	-36.3	1.2	-28.8	-7.7
429	Enclosed	WI	0	0	8	3	67	13	292	15	88	3	3	12.5	29.0	-38.7	0.2	-32.3	-6.6
499	Open-Field	WI	1	1	29	13	315	53	835	28	123	2	5	13.5	28.6	-35.1	0.1	-27.6	-7.7
698	Open-Field	WI	3	1	15	6	219	58	1108	46	209	4	5	13.6	28.9	-34.9	0.1	-25.8	-9.3
313	Enclosed	WV	1	1	8	4	104	20	373	17	81	2	4	12.8	28.9	-44.6	0.1	-36.9	-7.9
653	Enclosed	WV	1	1	11	4	119	27	606	30	209	5	7	15.4	29.2	-	-	-	-
656	Open-Field	WV	9	3	32	9	282	54	1112	42	173	3	4	14.6	28.8	-36.0	0.4	-26.5	-9.8

As reported in West et al., 2009b.

745
746

746

Table 2. Average concentrations, carbon preference indices, average chain lengths, and carbon isotope values of Cannabis inflorescence *n*-alkanes between the two growth environments

Cultivation Setting	Total *n*-Alkane Concentration ($\mu g\ g^{-1}$)	CPI	ACL	$\delta^{13}C_{n\text{-}C29}$ (‰, VPDB)	ε_{app} (‰, VPDB)
Enclosed	976 ± 432 (*22*)	12.6 ± 1.3 (*22*)	29.0 ± 0.1 (*22*)	-41.3 ± 8.2 (*15*)	-7.5 ± 0.9 (*15*)
Open-Field	1695 ± 1214 (*62*)	14.0 ± 2.0 (*62*)	28.8 ± 0.2 (*62*)	-36.2 ± 1.5 (*57*)	-8.5 ± 1.1 (*57*)

747
748
749

749 **Graphical Abstract:**
750

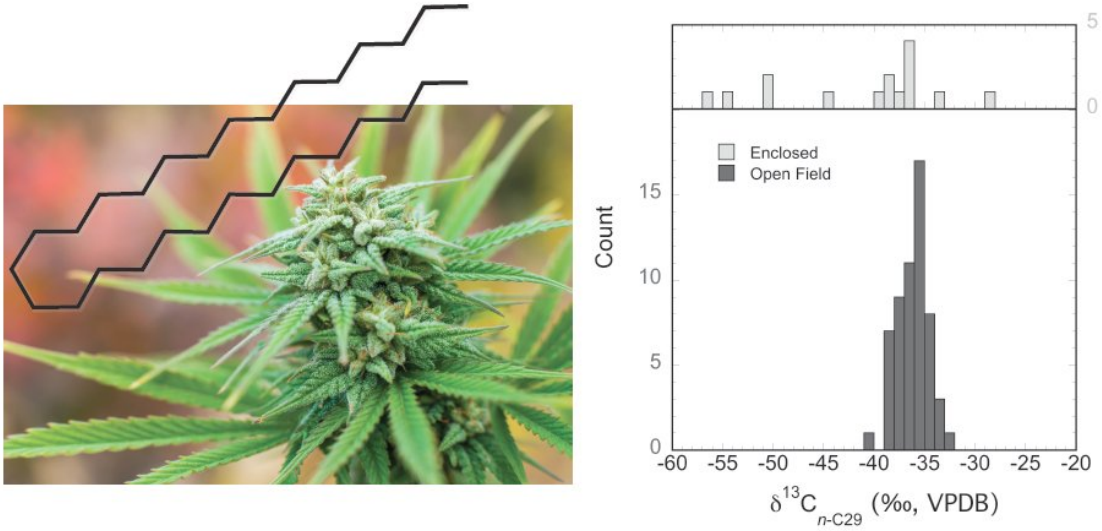

751
752
753

Figure 3

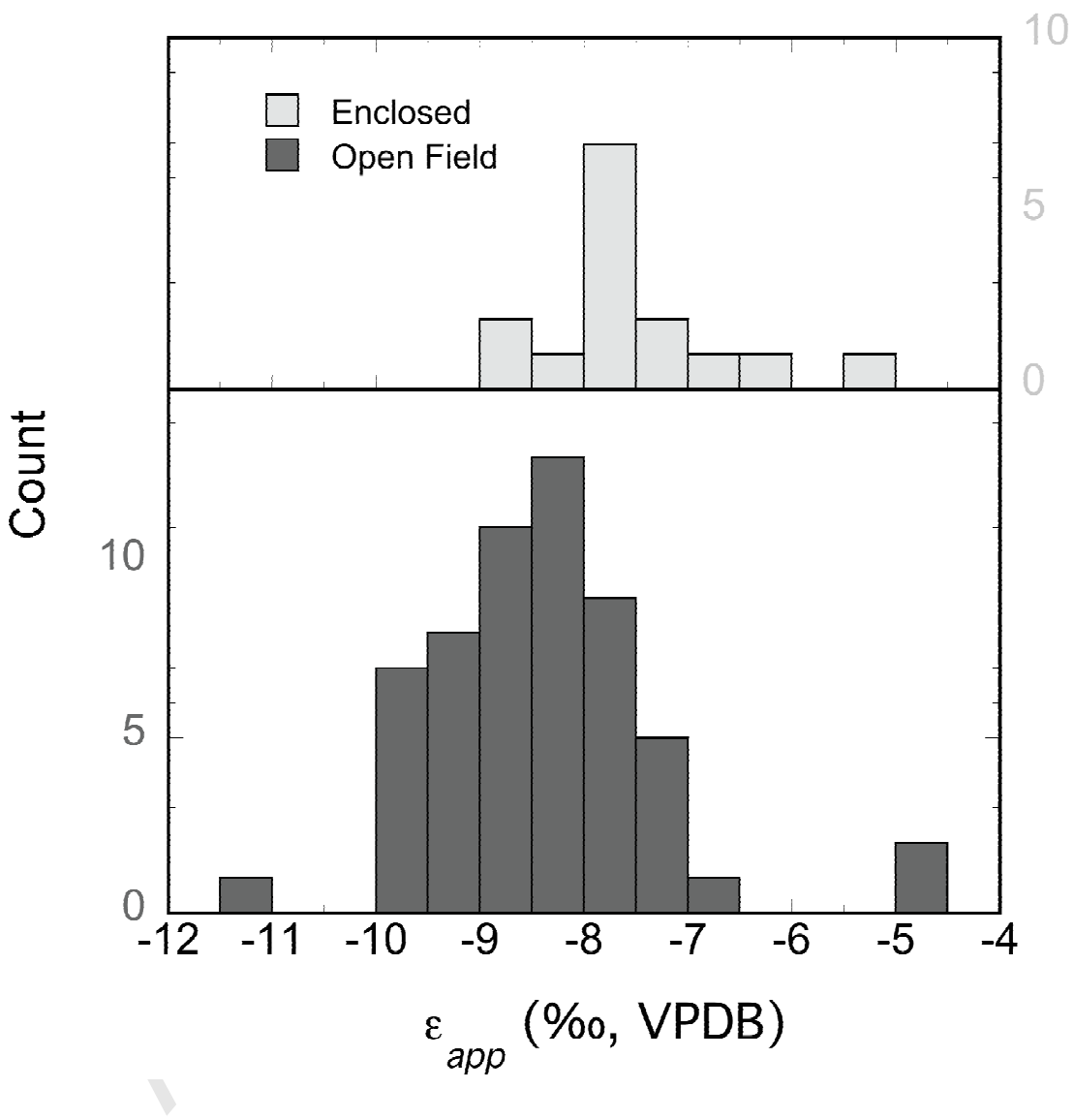

Figure 3. Histogram of the apparent fractionation (ε_{app}) between *n*-C_{29} extracted from inflorescence versus bulk inflorescence measured for the same sample. Specimens grown

762 within enclosed environments are shown in light grey, while plants grown in field
763 environments are shown in dark grey.
764